

1

Supplementary Information

2

3 Synergy of nitrogen vacancies and partially broken hydrogen bonds in
4 graphitic carbon nitride for superior photocatalytic hydrogen evolution
5 under visible light

6

7

8 Haifeng Dang^{a,*}, Suhua Mao^{a,b}, Qi Li^b, Mengyun Li^a, Mengmeng Shao^a, Wenlong Wang^a,
9 Quanbing Liu^b

10

11 ^a School of Materials Science and Engineering, Dongguan University of Technology, Dongguan
12 523808, PR China

13 ^b School of Chemical Engineering and Light Industry, Guangdong University of Technology,
14 Guangzhou 510006, PR China

15

16

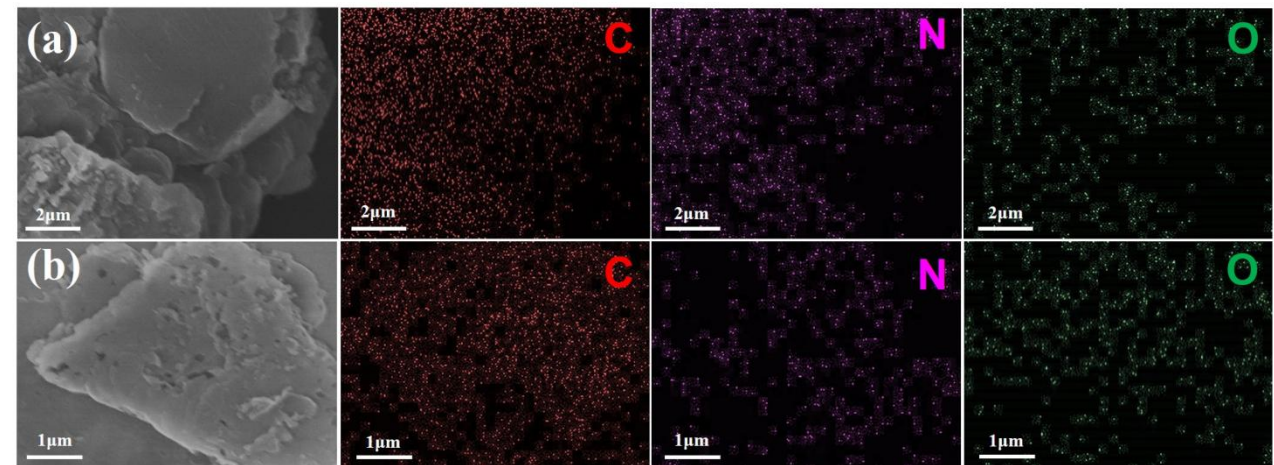
17

* Corresponding author.

E-mail: danghf@dgut.edu.cn (H. Dang).

18

19

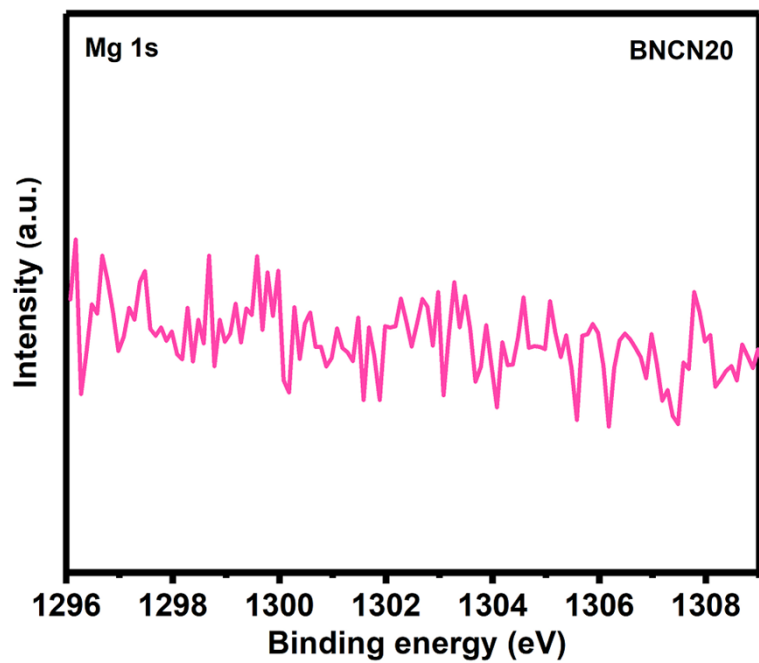


20
21 **Fig. S1** SEM and elements mapping images of (a) HCN and (b) BCN.

22

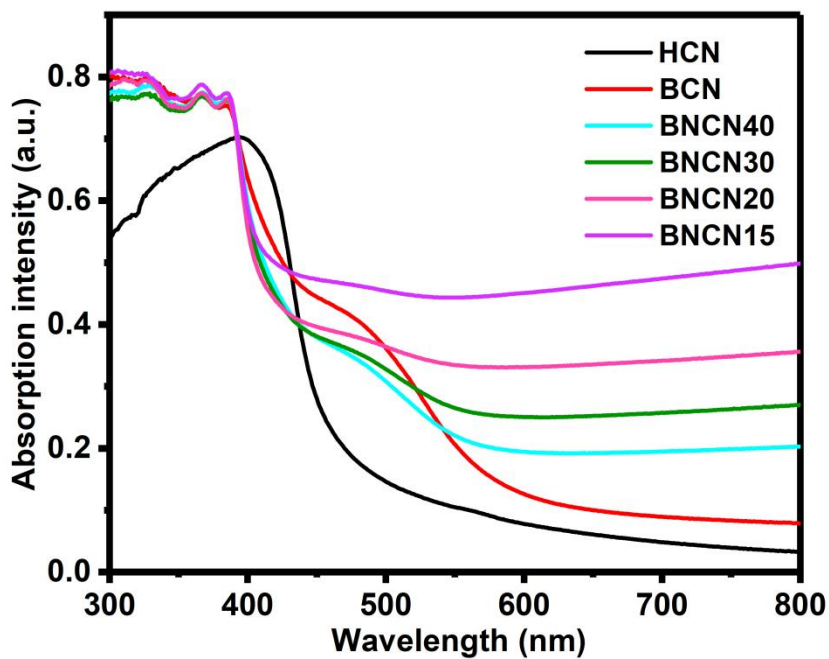
23

24



32
33 **Fig. S2** Mg 1s XPS of BNCN20 sample.

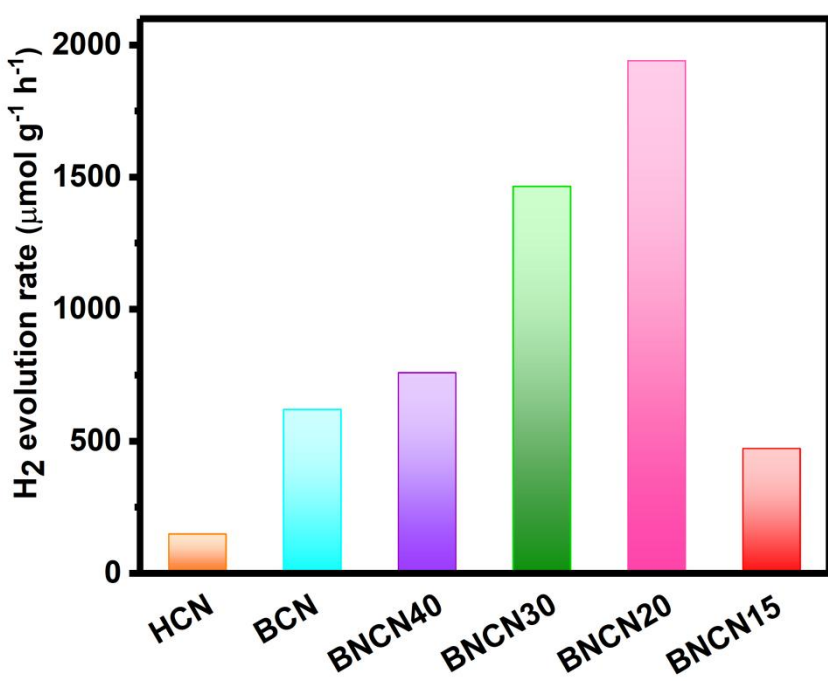
34



35

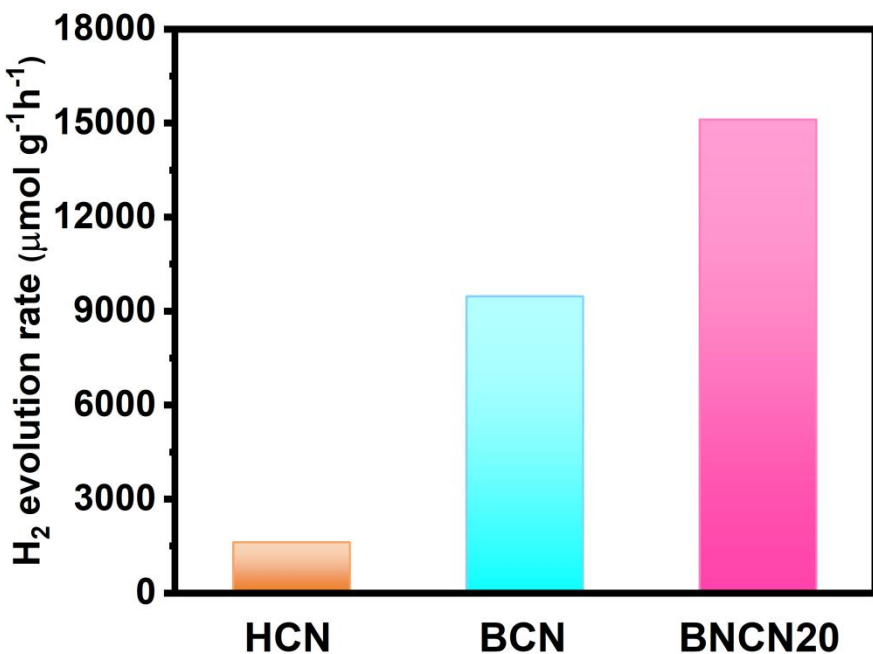
36 **Fig. S3** UV-visible absorption spectroscopy of HCN, BCN and BNCNx with different weight ratios
37 (40~15).

38



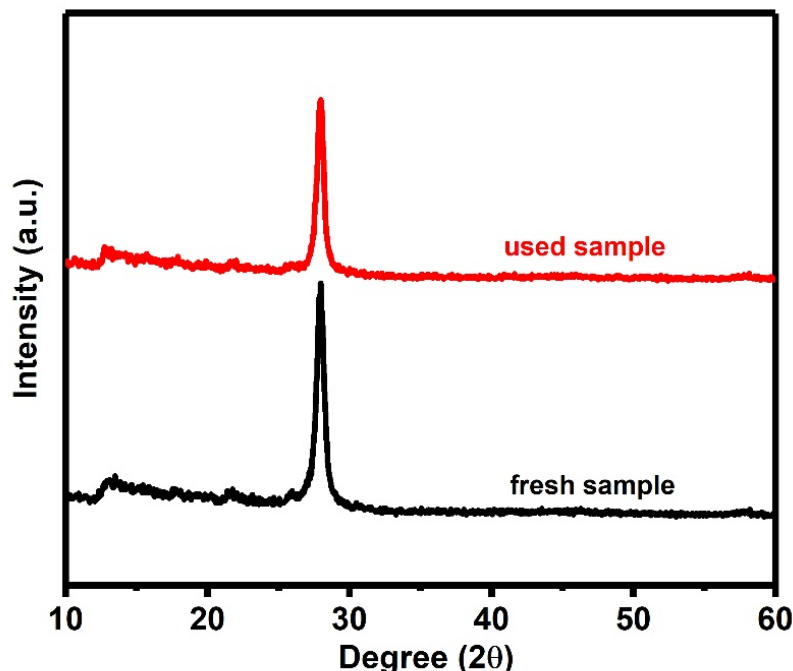
39

40 **Fig. S4** Photocatalytic hydrogen production of HCN, BCN and BNCNx with different weight ratios
41 (40~15) under visible-light irradiation ($\lambda > 400$ nm).



47

48 **Fig. S6** XRD patterns of the BNCN20 before and after four circulating runs of hydrogen production.



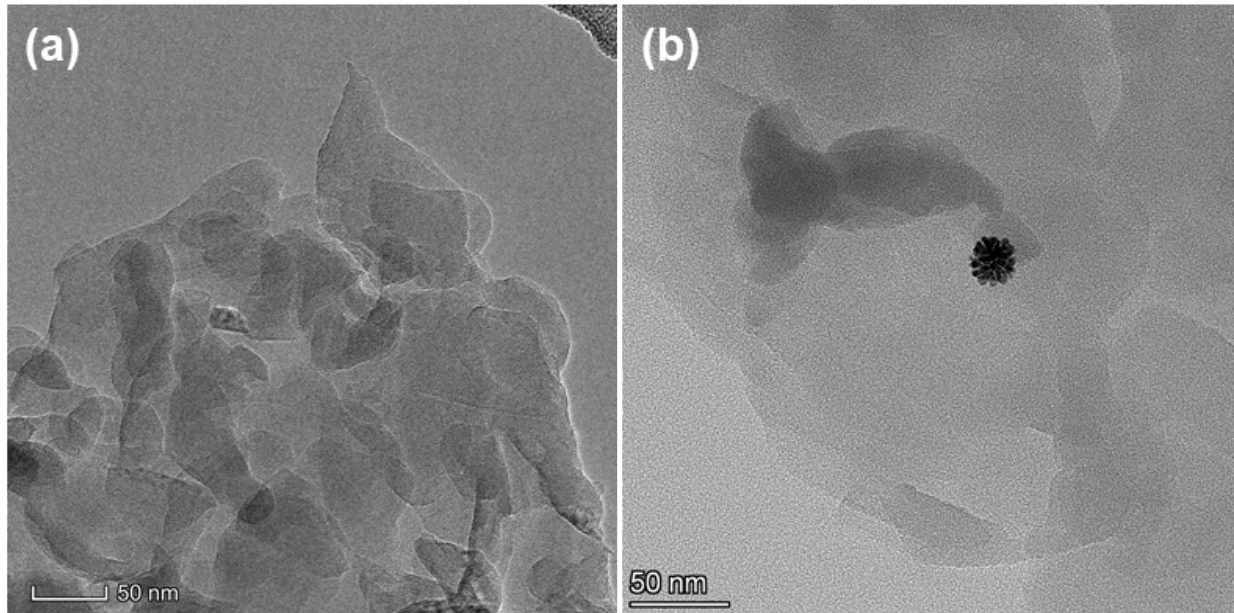


Fig. S7 TEM image of the BNCN20 after four circulating runs of hydrogen production.

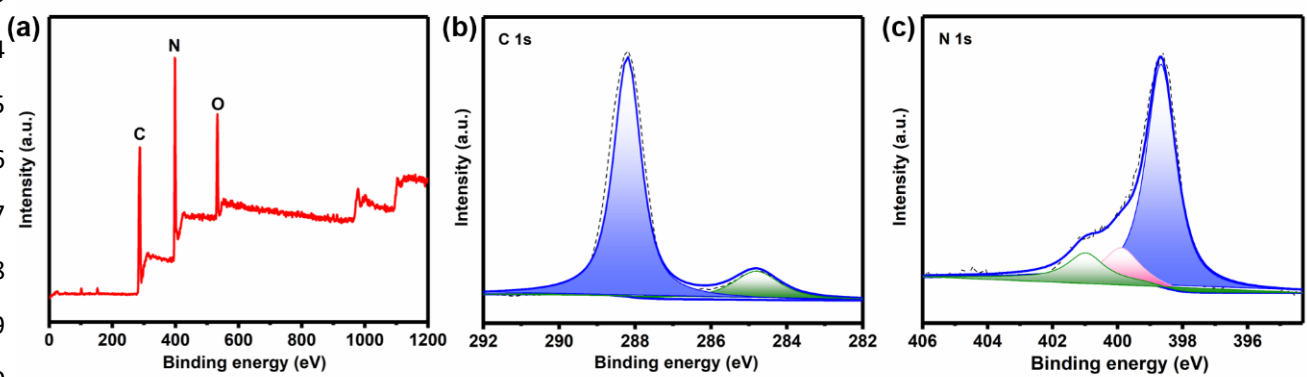


Fig. S8 XPS spectra of the used BNCN20: (a) Survey, (b) N1s, and (c) N1s.

Table S1. Summarized N_2 adsorption-desorption isotherm data for HCN, BCN, and BNCN.

| Sample | S_{BET} [$\text{m}^2 \text{ g}^{-1}$] | S_{ext}^1 [$\text{m}^2 \text{ g}^{-1}$] | S_{micro} [$\text{m}^2 \text{ g}^{-1}$] | V_{tol}^2 [$\text{cm}^3 \text{ g}^{-1}$] | V_{micro} [$\text{cm}^3 \text{ g}^{-1}$] | V_{meso}^3 [$\text{cm}^3 \text{ g}^{-1}$] |
|--------|---|---|---|--|--|---|
| HCN | 3.2342 | 4.3566 | — | 0.06054 | — | 0.06054 |
| BCN | 28.6470 | 20.8378 | 7.8092 | 0.195879 | 0.003322 | 0.192557 |
| BNCN20 | 40.3037 | 36.0487 | 4.2549 | 0.2564 | 0.001959 | 0.254402 |

66 1 Determined from t-plot method.

67 2 Determined from adsorbed volume at $P/P_0 = 0.98$.

68 3 $V_{\text{meso}}=V_{\text{tot}}-V_{\text{micro}}$.

69

70

71 **Table S2.** The deconvolution results of C 1s and N 1s XPS spectra of HCN, BCN, and BNCN20.

72

| Samples | C (eV) | | | N (eV) | | | |
|---------|--------|---------|-----------------|-----------------|-----------------|----------------------------------|----------------------------------|
| | N-C=N | C-C/C=C | NH _x | N _{3C} | N _{2C} | NH _x /N _{3C} | N _{2C} /N _{3C} |
| HCN | 288.2 | 284.8 | 401.0 | 400.1 | 398.5 | 0.88 | 7.89 |
| BCN | 288.2 | 284.8 | 401.0 | 400.1 | 398.5 | 0.77 | 7.85 |
| BNCN20 | 288.2 | 284.8 | 401.0 | 399.8 | 398.5 | 0.68 | 5.98 |

73

74

75

76 **Table S3.** Relative quantification of the Solid-State MAS ¹³C NMR spectra of HCN, BCN and

77 BNCN20 samples.

78

| Sample | C3/C2 |
|--------|-------|
| HCN | 1.49 |
| BCN | 1.42 |
| BNCN20 | 1.92 |

79

80

81 **Table S4.** The apparent quantum efficiency of HCN, BCN and BNCN20 (loaded with 1.5wt% Pt
82 by in-situ photoreduction) under different wavelengths.

83

| AQE \ Sample | 405 nm | 420 nm | 435 nm | 450 nm | 475 nm | 500 nm |
|--------------|--------|--------|--------|--------|--------|--------|
| HCN | 0.68% | 0.40% | 0.12% | 0 | 0 | 0 |
| BCN | 2.12% | 2.29% | 3.19% | 2.84% | 0 | 0 |
| BNCN20 | 9.58% | 8.57% | 8.38% | 4.21% | 2.91% | 0 |

84

85

86

87

88 **References**

- 89 [S1] J. Zhang, S. Gong, N. Mahmood, L. Pan, X. Zhang and J. Zou, Oxygen-doped nanoporous
90 carbon nitride via water-based homogeneous supramolecular assembly for photocatalytic
91 hydrogen evolution. *Appl. Catal. B*, 2018, **221**, 9-16.
- 92 [S2] K. Schwinghammer, M.B. Mesch, V. Duppel, C. Ziegler, J. Senker and B.V. Lotsch,
93 Crystalline carbon nitride nanosheets for improved visible-light hydrogen evolution. *J. Am.
94 Chem. Soc.*, 2014, **136**, 1730-1733.
- 95 [S3] Y. Guo, J. Li, Y. Yuan, L. Li, M. Zhang, C. Zhou and Z. Lin, A rapid microwave-assisted
96 thermolysis route to highly crystalline carbon nitrides for efficient hydrogen generation. *Angew.
97 Chem. Int. Ed.*, 2016, **55**, 14693-14697.

- 98 [S4] H. Yu, R. Shi, Y. Zhao, T. Bian, Y. Zhao, C. Zhou, G.I.N. Waterhouse, L. Wu, C. Tung and T.
99 Zhang, Alkali-assisted synthesis of nitrogen deficient graphitic carbon nitride with tunable
100 band structures for efficient visible-light-driven hydrogen evolution. *Adv. Mater.*, 2017, **29**,
101 1605148.
- 102 [S5] D. Zhang, Y. Guo and Z. Zhao, Porous defect-modified graphitic carbon nitride via a facile
103 one-step approach with significantly enhanced photocatalytic hydrogen evolution under visible
104 light irradiation. *Appl. Catal. B*, 2018, **226**, 1-9.
- 105 [S6] Y. Kang, Y. Yang, L. Yin, X. Kang, L. Wang, G. Liu and H. Cheng, Selective breaking of
106 hydrogen bonds of layered carbon nitride for visible light photocatalysis. *Adv. Mater.*, 2016, **28**,
107 6471-6477.
- 108 [S7] B. Li, Y. Si, B. Zhou, Q. Fang, Y. Li, W. Huang, W. Hu, A. Pan, X. Fan and G. Huang,
109 Doping-induced hydrogen-bond engineering in polymeric carbon nitride to significantly boost
110 the photocatalytic H₂ evolution performance. *ACS Appl. Mater. Interfaces*, 2019, **11**, 17341-
111 17349.
- 112 [S8] J. Yang, Y. Liang, K. Li, G. Yang, K. Wang, R. Xu and X. Xie, One-step synthesis of novel K⁺
113 and cyano groups decorated triazine-/heptazine-based g-C₃N₄ tubular homojunctions for
114 boosting photocatalytic H₂ evolution. *Appl. Catal. B*, 2020, **262**, 118252.
- 115 [S9] W. Iqbal, B. Qiu, Q. Zhu, M. Xing and J. Zhang, Self-modified breaking hydrogen bonds to
116 highly crystalline graphitic carbon nitrides nanosheets for drastically enhanced hydrogen
117 production. *Appl. Catal. B*, 2018, **232**, 306-313.